

Identifying anatomical structures on ultrasound: assistive artificial intelligence in ultrasound-guided regional anesthesia

James Bowness^{1,2}  | Ourania Varsou³ | Lloyd Turbitt⁴ | David Burkett-St Laurent⁵

¹Oxford Simulation, Teaching and Research Centre, University of Oxford, Oxford, UK

²Department of Anaesthesia, Aneurin Bevan University Health Board, Newport, UK

³Anatomy Facility, School of Life Sciences, University of Glasgow, Glasgow, UK

⁴Department of Anaesthesia, Belfast Health and Social Care Trust, Belfast, UK

⁵Department of Anaesthesia, Royal Cornwall Hospitals NHS Trust, Truro, UK

Correspondence

James Bowness, OxSTaR Centre, Nuffield Division of Anaesthetics, Nuffield Department of Clinical Neurosciences, John Radcliffe Hospital, Oxford, OX3 9D, UK.
Email: james.bowness@jesus.ox.ac.uk

Abstract

Ultrasound-guided regional anesthesia involves visualizing sono-anatomy to guide needle insertion and the perineural injection of local anesthetic. Anatomical knowledge and recognition of anatomical structures on ultrasound are known to be imperfect amongst anesthesiologists. This investigation evaluates the performance of an assistive artificial intelligence (AI) system in aiding the identification of anatomical structures on ultrasound. Three independent experts in regional anesthesia reviewed 40 ultrasound scans of seven body regions. Unmodified ultrasound videos were presented side-by-side with AI-highlighted ultrasound videos. Experts rated the overall system performance, ascertained whether highlighting helped identify specific anatomical structures, and provided opinion on whether it would help confirm the correct ultrasound view to a less experienced practitioner. Two hundred and seventy-five assessments were performed (five videos contained inadequate views); mean highlighting scores ranged from 7.87 to 8.69 (out of 10). The Kruskal–Wallis H -test showed a statistically significant difference in the overall performance rating ($\chi^2[6] = 36.719$, asymptotic $p < 0.001$); regions containing a prominent vascular landmark ranked most highly. AI-highlighting was helpful in identifying specific anatomical structures in 1330/1334 cases (99.7%) and for confirming the correct ultrasound view in 273/275 scans (99.3%). These data demonstrate the clinical utility of an assistive AI system in aiding the identification of anatomical structures on ultrasound during ultrasound-guided regional anesthesia. Whilst further evaluation must follow, such technology may present an opportunity to enhance clinical practice and energize the important field of clinical anatomy amongst clinicians.

KEYWORDS

artificial intelligence, regional anesthesia, sono-anatomy, ultrasound

Presentation

This work has not been presented.

This is an open access article under the terms of the Creative Commons Attribution License, which permits use, distribution and reproduction in any medium, provided the original work is properly cited.

© 2021 The Authors. *Clinical Anatomy* published by Wiley Periodicals LLC on behalf of American Association of Clinical Anatomists.

“Anatomical knowledge is clearly relevant to the invasive procedures undertaken in anaesthetic practice, and possibly vital to the interpretation of images generated by ultrasound devices.”

(Dr David Mulvey, Chair of the Royal College of Anaesthetists Short Answer Question Group; Report on the FRCA Short Answer Question Paper, March 2014)

1 | INTRODUCTION

Ultrasound-guided regional anesthesia (UGRA) involves visualizing sono-anatomy in real time to guide needle insertion and the subsequent perineural deposition of local anesthetic. This provides selective blockade of sensory and motor stimuli conveyed by peripheral nerves in order to produce anesthesia and/or analgesia of the affected region. Ultrasound has become the predominant technique to guide the performance of regional anesthesia (Helen et al., 2015; Munimara & McLeod, 2015). Its use has several potential advantages, including visualization of the relevant anatomical structures (Henderson & Dolan, 2016; Hutton et al., 2018). This requires a good understanding of the sono-anatomy and sonographic visualization of the area of interest for safe and effective conduct (Henderson & Dolan, 2016; Sites et al., 2009; Taylor & Grant, 2019). Despite this, anatomical knowledge amongst anesthesiologists may be flawed, as demonstrated by the following report on the Fellowship of the Royal College of Anaesthetists (FRCA) examination (Tremlett, 2014):

“The lack of even basic knowledge of anatomy has been identified over a number of years, reflecting the fall in teaching of basic sciences at undergraduate level. The need to learn and test anatomy remains of fundamental importance particularly with the resurgence of Regional Anaesthesia in the UK in the last decade. Anaesthetists are commonly placing needles in a range of sites for local anaesthetic blocks and must understand key structures the needles may approach/hit.”

We have previously discussed the potential for variable recognition of anatomical structures on ultrasound, even by experienced regional anesthesiologists (Bowness, Turnbull, Taylor, Halcrow, Chisholm, et al., 2019; Bowness, Turnbull, Taylor, Halcrow, Raju, et al., 2019). Based on this information, we presented the case for the use of assistive artificial intelligence (AI) technology to facilitate the recognition of anatomical structures in UGRA (Bowness et al., 2020). This concept has also been proposed by other groups, both for UGRA (Alkhatib et al., 2019; Huang et al., 2019) and central neuraxial blockade (spinal and epidural) (Oh et al., 2019; Smistad et al., 2018; Tran & Rohling, 2010).

The current investigation presents an initial evaluation of an AI system called *ScanNav Anatomy Peripheral Nerve Block* (also known as *ScanNav Anatomy PNB* and formerly known as *AnatomyGuide*; Intelligent Ultrasound Ltd [IUL], Cardiff, UK). This system uses deep convolutional neural networks based on the U-Net architecture (Ronneberger et al., 2015) to perform semantic segmentation of the input ultrasound videos. A separate network was created for the anatomical region relevant to each specific peripheral nerve block.

Ultrasound scans of the region were recorded and manually segmented to identify the specific anatomical structures relevant to regional anesthesia. Through this process the neural network learns to perform segmentation (color overlay highlighting) of the anatomical structures on ultrasound scans in real time, to aid in identifying anatomy during UGRA. To our knowledge, this is the first investigation which presents performance of a system over multiple anatomical regions, from a clinical perspective.

The primary aims were to assess, in the opinion of expert regional anesthesiologists, the following:

- Overall performance of the system when highlighting structures on ultrasound scans
- The benefit of highlighting on the identification of individual structures on ultrasound scans
- The benefit of highlighting in aiding confirmation of the correct ultrasound view to a less experienced practitioner.

2 | MATERIALS AND METHODS

2.1 | Study registration, ethical approval and participant recruitment

Ultrasound scans used for this investigation were collected via four separate studies, all registered with www.clinicaltrials.gov in advance of commencing participant recruitment. All participants were given a participant information sheet and provided written consent prior to commencing data collection.

For study ML2018_AG_02 (NCT03647618), ethical approval was provided by Newcastle and North Tyneside Research Ethics Committee 1 (REC reference number 18/NE/0323) for the involvement of patients at Aneurin Bevan University Health Board (ABUHB). One hundred and forty-four anonymized ultrasound videos were recorded from patients undergoing treatment at four clinical centers within ABUHB: the Royal Gwent Hospital, Ystrad Mynach Hospital, St Woolos Hospital, and Nevill Hall Hospital. All were undergoing UGRA as a planned part of their treatment, thus participation had no influence on their clinical care.

Additional studies were carried out to record data from 244 healthy volunteers:

- ML2018_AG_01: 103 participants, yielding 112 scan videos (NCT036543000)
- IU2019_AG_03: 42 participants, yielding 42 scan videos (NCT04040179)
- IU2020_AG_04: 99 participants, yielding 99 scan videos (NCT04277169)

Volunteers were recruited by placing advertisements around the University Hospital of Wales campus and by using social media. All potential volunteer participants were screened against the inclusion criteria detailed below:

- Age \geq 18 years
- Able to understand the participant information and provide written consent

2.2 | Ultrasound assessment

Basic demographic information was collected for all participants, including age, height, weight and BMI (available in Supplementary material S1). The regions scanned were relevant to specific peripheral nerve blocks as follows:

- Interscalene-supraclavicular level brachial plexus (anterolateral neck, from the level of the C5 vertebra inferiorly to the supraclavicular fossa)
- Axillary level brachial plexus (medial arm, adjacent to the anterior axillary fold)
- Erector spinae plane (thoracic region of the back; focusing on a plane deep to the erector spinae muscle group and superficial to the lateral margins of the thoracic transverse processes/ribs)
- Rectus sheath (anterior abdominal wall, between the level of the xiphisternum and umbilicus)
- Suprainguinal fascia iliaca (fascia over iliacus muscle, medial to the point of the anterior superior iliac spine)
- Adductor canal (anteromedial thigh, just proximal to the midpoint between the anterior superior iliac spine and the apex of the patella)
- Popliteal level sciatic nerve (lateral aspect of the popliteal fossa, proximal to the popliteal skin crease at the point of separation of the tibial and common peroneal [fibular] components)

Ultrasound assessments of ABUHB patients undergoing UGRA procedures were performed by the anesthesiologist performing the procedure. Scanning of healthy volunteers was performed by two qualified sonographers. All volunteers were scanned for multiple regions, carried out using high-frequency linear array ultrasound transducer probes on one of five ultrasound machines (GE Voluson E8, SonoSite Edge, Sonoscape p50, SonoSite X-Porte, SonixTouch Research). For the scanning of healthy volunteers, the region of interest was scanned as would be done in clinical practice, to assess the sono-anatomy and identify the optimal block site (correct ultrasound view prior to introducing the needle for local anesthetic injection).

Data from all studies were aggregated. From these, 40 scans from each region were selected at random for this investigation.

2.3 | ScanNav anatomy peripheral nerve block highlighting

ScanNav Anatomy PNB performs highlighting for the following structures in each block region: (Figure 1 and supplementary material B–H):

- Interscalene-supraclavicular level brachial plexus: subclavian artery, brachial plexus nerves (roots – trunks/divisions), sternocleidomastoid/anterior scalene muscles, first rib, pleura

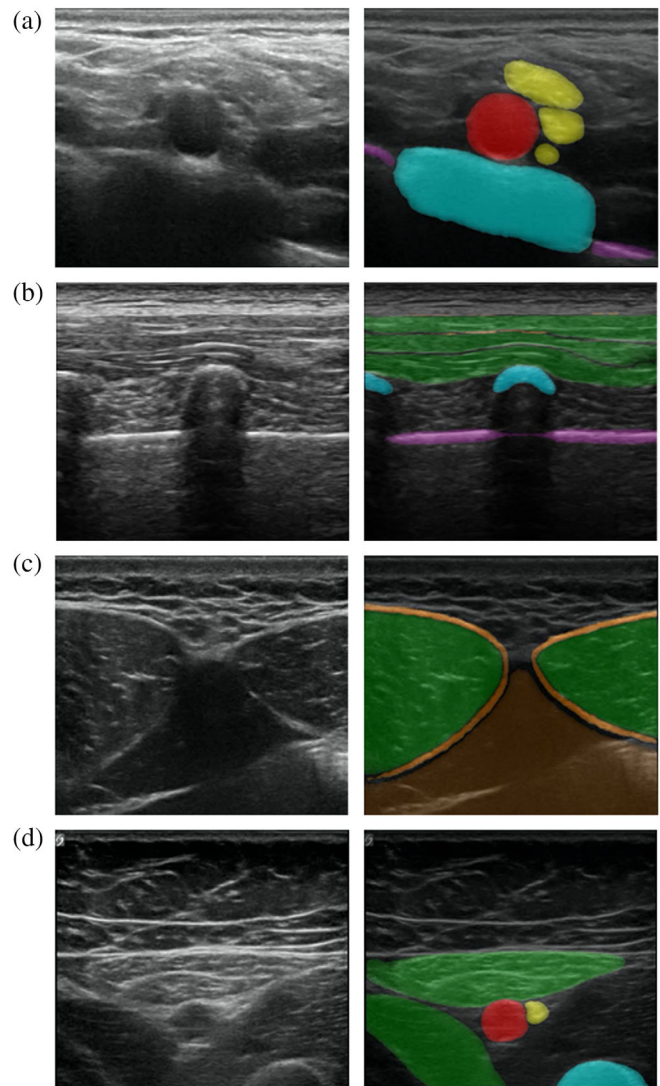


FIGURE 1 Still images taken from ultrasound videos labeled by *ScanNav Anatomy PNB*

- (a) Supraclavicular level brachial plexus: subclavian artery (red), brachial plexus nerves (yellow), first rib (blue), pleura (purple).
 (b) Erector spinae plane (thoracic region): trapezius/rhomboid/erector spinae (group) muscles (green), vertebral transverse process/rib (blue), pleura (purple).
 (c) Rectus sheath: rectus abdominis muscle (green), rectus sheath (orange), peritoneal contents (brown).
 (d) Adductor canal: femoral artery (red), saphenous nerve (yellow), sartorius/adductor longus (green), femur (blue) [Color figure can be viewed at wileyonlinelibrary.com]

- Axillary level brachial plexus: axillary artery, radial/median/ulnar/musculocutaneous nerve, fascia over conjoint tendon of latissimus dorsi/teres major, humerus
- Erector spinae plane: trapezius/rhomboid/erector spinae (group) muscles, ribs/thoracic vertebral transverse processes, pleura
- Rectus sheath: rectus abdominis/transversus abdominis muscles, rectus sheath, peritoneum/peritoneal contents
- Suprainguinal fascia iliaca: deep circumflex iliac artery, iliacus muscle, fascia iliaca, ilium (anterior superior iliac spine)

- Adductor canal: femoral artery, saphenous nerve, sartorius muscle, adductor longus, femur
- Popliteal level sciatic nerve: popliteal artery, sciatic/tibial/common peroneal (fibular) nerves.

2.4 | Expert assessment

Three independent experts in regional anesthesia (with no involvement in the design of *ScanNav Anatomy PNB*) reviewed 40 videos of each block region. One expert is a consultant anesthetist in the UK and two are attending anesthesiologists in the USA. All have completed advanced training in regional anesthesia through a postgraduate fellowship and regularly conducts anesthesia using advanced UGRA techniques. The original ultrasound video was presented side-by-side with the ultrasound video overlaid by AI highlighting. The experts were asked to answer the following questions for each one:

- Does the video contain clinically relevant images for this block area? [Y/N]
- Rate the overall highlighting performance on a scale of 0–10? [0 – very poor, 10 – excellent]
- Did the highlighting help identify the [insert structure name]? [Y/N]
- Would the highlighting help confirm the correct ultrasound view to a less experienced practitioner? [Y/N]

For the purposes of this study, a less experienced practitioner refers to an individual qualified to perform UGRA techniques, but lacks extensive experience/advanced training and does not identify as an expert or regularly undertake/teach UGRA techniques. This group is predominantly composed of anesthesiologists who have not completed advanced training in regional anesthesia, but may extend to clinicians in complimentary specialties (e.g. emergency medicine).

2.5 | Statistical analysis

Anonymized data were initially recorded in Microsoft Excel and transferred to SPSS version 27 (IBM Corp, 2020). Analysis was conducted by an independent researcher, not involved in data collection, to eliminate bias.

| | NeckBP | AxBP | ESP | RS | FI | AC | PopSN |
|--------|--------|-------|-------|-------|-------|-------|-------|
| Min | 5.33 | 5.33 | 6.33 | 5.67 | 6.33 | 5.67 | 5.67 |
| Max | 9.33 | 10.00 | 9.67 | 9.00 | 10.00 | 9.67 | 9.33 |
| St Dev | 1.017 | 0.981 | 0.666 | 0.816 | 0.812 | 0.698 | 0.867 |
| Mean | 7.89 | 8.43 | 8.10 | 7.87 | 8.42 | 8.69 | 8.09 |

Abbreviations: NeckBP: interscalene - supraclavicular level brachial plexus; Ax - axillary level brachial plexus; ESP: erector spinae plane; FI: suprainguinal fascia iliaca; RS: rectus sheath; AC: adductor canal; PopSN: popliteal level sciatic nerve).

If the majority answer to the first question “does the video contain clinically relevant images for this block area?” was “no”, the data relating to this video was not included in the analysis.

For ultrasound videos deemed to contain clinically relevant images, the mean of the three experts' rating was calculated and reported for the 0–10 overall clinical rating. For the three experts' answers to the dichotomous [Y/N] questions, the predominant response was determined and reported.

Descriptive statistics were used to present the overall clinical performance of the system and identification of specific structures. The Kruskal-Wallis *H*-test was used to assess for statistically significant differences of the highlighting performance rating between different block regions, with asymptotic exact *p* values reported. This test was chosen due to the ordinal nature of the 0–10 rating scale. For the post-hoc analysis, the Dunn's procedure was used for pairwise comparisons with a Bonferroni correction ($p < 0.05$) and adjusted *p* values reported.

3 | RESULTS

Five of the 40 erector spinae plane ultrasound videos were deemed not to contain clinically relevant images; thus the analysis of this region was based on responses when assessing the remaining 35 videos. In the other six regions all 40 videos were included. Thus, a total of 275 ultrasound videos were assessed.

A summary of the overall highlighting performance for each block area is presented in Table 1. As can be seen, the mean highlighting score for all regions ranged from 7.87 to 8.69 (out of 10). The two lowest scoring regions were the rectus sheath and the interscalene - supraclavicular level brachial plexus (7.87 and 7.89). The two highest scoring regions were the axillary level brachial plexus and the adductor canal (8.43 and 8.69).

When comparing one region to the other, the Kruskal-Wallis *H*-test showed a highly statistically significant difference in the overall highlighting performance rating between different blocks ($\chi^2[6] = 36.719$, asymptotic $p < 0.001$). The mean rank, in ascending order, was:

- 102.14 for rectus sheath
- 114.19 for interscalene - supraclavicular level brachial plexus
- 116.94 for erector spinae plane
- 125.09 for popliteal level sciatic nerve

TABLE 1 A summary of the overall highlighting performance for each block area

- 154.82 for suprainguinal fascia iliaca
- 163.64 for axillary level brachial plexus
- 186.55 for adductor canal.

The Dunn's procedure showed a statistically significant difference between specific high and low-ranked blocks. Rectus sheath and axillary level brachial plexus (61.500, $p = 0.01$ adjusted by Bonferroni correction), as well as popliteal level sciatic nerve and adductor canal (61.463, $p = 0.01$ adjusted by Bonferroni correction). A highly statistically significant difference was also seen between the rectus sheath and adductor canal (84.413, $p < 0.001$ adjusted by Bonferroni correction), interscalene - supraclavicular level brachial plexus and adductor canal (72.363, $p = 0.001$ adjusted by Bonferroni correction), and the erector spinae plane and adductor canal (69.607, $p = 0.003$ adjusted by Bonferroni correction).

As seen in Table 2, highlighting was considered helpful in the identification of specific structures in 95–100% of cases. The highlighting, in the opinion of experts, was considered helpful in 100% of cases for 31 of the 34 structures. The least helpful highlighting was for the musculocutaneous nerve (helpful in 38/40 cases; 95%), followed by the deep circumflex iliac artery (37/38; 97.4%), then the popliteal artery (39/40; 97.5%).

Expert opinion on whether highlighting would assist in confirmation of the correct ultrasound view to a less experienced practitioner was 40/40 or 35/35 (100%; by majority view for each ultrasound scan) for five of the seven regions assessed (see Table 3). Ultrasound scans of the interscalene - supraclavicular and axillary levels of the brachial plexus both scored as helpful in 39/40 (97.5%) of cases.

4 | DISCUSSION

This paper reports a clinician-rated assessment of the utility of an assistive AI system to facilitate the identification of key anatomical structures on ultrasound for the purposes of UGRA. As far as the authors are aware, this is the first assessment of AI technology in this field which presents the evaluation from the perspective of the end user.

Three independent experts in regional anesthesia concluded that the overall performance of system highlighting, ranked 0 (very poor) – 10 (excellent), was at minimum 7.87. Statistically significant differences in performance for different block regions were noted, in particular between the rectus sheath and interscalene – supraclavicular level brachial plexus regions (lowest ranked), and the axillary level brachial plexus and adductor canal regions (highest ranked). It is notable that two of the three lowest ranked regions do not contain major vascular landmarks and are plane blocks. In contrast, both of the highest ranked regions contain vascular and bony landmarks, as well as distinct nerves that are targeted.

Expert opinion indicated that this highlighting would help identify specific structures and confirm the correct ultrasound view to a less experienced practitioner. Of a total of 1334 assessments of specific

anatomical structures, the highlighting was considered helpful in their identification for 1330 (99.7%). From a total of 275 assessments with respect to confirming the correct view, only two (<1%) were not deemed to be helpful. As noted earlier, recognition of salient anatomical structures on ultrasound and confirming the correct view are essential components of UGRA.

This analysis has demonstrated promising results for the potential of *ScanNav Anatomy PNB* to aid in the identification of anatomical structures on ultrasound and assist non-expert operators in identifying the correct ultrasound view to perform the block. Potential deficiencies in anatomical knowledge are apparent amongst FRCA candidates (anesthesiologists up to 5 years through a seven-year anesthesiology training programme in the UK, at least 7 years after graduation from medical school). These deficiencies may be compounded by the interface of anatomical knowledge with ultrasound image interpretation. Therefore, such assistive AI approaches could be of clinical benefit when performing invasive procedures on patients: improving interpretation of sono-anatomy to aid the success of clinical procedures, and contribute positively to patient safety by simplifying and standardizing one major aspect of UGRA. This approach also presents an opportunity to adopt innovation to rejuvenate the field of clinical anatomy. Artificial Intelligence technology may enhance accessibility and learning opportunities for clinicians who engage in clinical anatomy on a regular basis, but require further anatomical knowledge or skills in sono-anatomy interpretation.

There has been a recent move to increase the use, and standardize practice, of UGRA amongst non-experts in the UK (Turbitt et al., 2020). The utilization of assistive technology may facilitate this approach and enhance consistency of ultrasound interpretation compared to human performance. There is potential for application of this system in other specialties, for example emergency medicine. Emergency medicine physicians perform UGRA on a less frequent basis than anesthesiologists, hence may be less confident in recognizing key structures on ultrasound, and so may benefit from this standardized assistive technology. Furthermore, this approach may support other image-guided interventional specialties/practice, such as interventional radiology.

This clinically orientated evaluation of AI anatomy identification is a novel approach to assessing such technology, as it is taken from the point of the end-user. Statistical techniques to provide a quantitative assessment of system performance have been used in prior publications, such as Intersection over Union (Huang et al., 2019) and the Dice co-efficient (Smistad et al., 2018). However, as there has been little work done to determine the clinical utility of any given threshold in these metrics, the approach in this investigation emphasizes the ultimate need for the clinician to recognize the salient anatomical structures (which the system is designed to aid). Furthermore, such metrics evaluate still image labelling, whilst the practice of UGRA relies on the interpretation of ultrasound videos in real time. Therefore, whilst evaluation of still frame is one component, the entire ultrasound video must also be considered as it is in clinical practice.

The authors acknowledge that this is a preliminary and subjective assessment of the system. For example, there was a statistically

TABLE 2 Expert opinion on whether highlighting helped identify individual structures

| Structure | Yes | No |
|---|-----------------|--------------|
| Interscalene - Supraclavicular Level Brachial Plexus | | |
| Subclavian artery | 40/40 (100%) | 0/40 (0%) |
| Brachial plexus nerves | 40/40 (100%) | 0/40 (0%) |
| Sternocleidomastoid muscle | 40/40 (100%) | 0/40 (0%) |
| Scalenus anterior muscle | 40/40 (100%) | 0/40 (0%) |
| First rib | 40/40 (100%) | 0/40 (0%) |
| Pleura | 40/40 (100%) | 0/40 (0%) |
| Total (for block) | 240/240 (100%) | 0/240 (0%) |
| Axillary Level Brachial Plexus | | |
| Axillary artery | 40/40 (100%) | 0/40 (0%) |
| Radial nerve | 40/40 (100%) | 0/40 (0%) |
| Median nerve | 40/40 (100%) | 0/40 (0%) |
| Ulnar nerve | 40/40 (100%) | 0/40 (0%) |
| Musculocutaneous nerve | 38/40 (95%) | 2/40 (5%) |
| Fascia (conjoint tendon) | 40/40 (100%) | 0/40 (0%) |
| Humerus | 40/40 (100%) | 0/40 (0%) |
| Total (for block) | 278/280 (99.3%) | 2/280 (0.7%) |
| Erector Spinae Plane | | |
| ^b Muscle layer (Trapezius, rhomboid, erector spinae) | 35/35 (100%) | 0/35 (0%) |
| ^b Ribs | 35/35 (100%) | 0/35 (0%) |
| ^b Transverse process | 35/35 (100%) | 0/35 (0%) |
| ^b Pleura | 35/35 (100%) | 0/35 (0%) |
| Total (for block) | 140/140 (100%) | 0/140 (0%) |
| Rectus Sheath | | |
| Rectus abdominis muscle | 40/40 (100%) | 0/40 (0%) |
| Transversus abdominis muscle | 40/40 (100%) | 0/40 (0%) |
| Rectus sheath | 40/40 (100%) | 0/40 (0%) |
| Peritoneum/peritoneal contents | 40/40 (100%) | 0/40 (0%) |
| Total (for block) | 160/160 (100%) | 0/160 (0%) |
| Suprainguinal Fascia Iliaca | | |
| ^a Deep circumflex iliac artery | 37/38 (97.4%) | 1/38 (2.6%) |
| Iliacus muscle | 40/40 (100%) | 0/40 (0%) |
| Fascia iliaca | 40/40 (100%) | 0/40 (0%) |
| Hip bone | 40/40 (100%) | 0/40 (0%) |
| Total (for block) | 157/158 (99.4%) | 1/158 (0.6%) |
| Adductor Canal | | |
| Femoral artery | 40/40 (100%) | 0/40 (0%) |
| Saphenous nerve | 40/40 (100%) | 0/40 (0%) |
| Sartorius muscle | 40/40 (100%) | 0/40 (0%) |
| Adductor longus muscle | 40/40 (100%) | 0/40 (0%) |
| ^a Femur | 38/38 (100%) | 0/38 (0%) |
| Total (for block) | 198/198 (100%) | 0/198 (0%) |
| Popliteal Level Sciatic Nerve | | |
| Popliteal artery | 39/40 (97.5%) | 1/40 (2.5%) |
| Sciatic nerve | 40/40 (100%) | 0/40 (0%) |
| ^a Tibial nerve | 39/39 (100%) | 0/39 (0%) |

TABLE 2 (Continued)

| Structure | Yes | No |
|--|-------------------|---------------|
| ^a Common peroneal (fibular) nerve | 39/39 (100%) | 0/39 (0%) |
| Total (for block) | 157 /158 (99.4%) | 1/158 (0.6%) |
| Total (for all structures/block) | 1330/1334 (99.7%) | 4/1334 (0.3%) |

^aTotal number of Y/N responses less than 40 in some rows because not all structures were present on all ultrasound videos.

^b35 ultrasound videos assessed for the erector spine plane region.

TABLE 3 Expert opinion on whether highlighting would help confirm the correct ultrasound view to a less experienced practitioner

| | NeckBP | AxBP | ESP | RS | FI | AC | PopSN |
|-------|---------------|---------------|--------------|--------------|--------------|--------------|--------------|
| Y (%) | 39/40 (97.5%) | 39/40 (97.5%) | 35/35 (100%) | 40/40 (100%) | 40/40 (100%) | 40/40 (100%) | 40/40 (100%) |
| N (%) | 1/40 (2.5%) | 1/40 (2.5%) | 0/35 (0%) | 0/40 (0%) | 0/40 (0%) | 0/40 (0%) | 0/40 (0%) |

Abbreviations: NeckBP: interscalene - supraclavicular level brachial plexus; Ax: axillary level brachial plexus; ESP: erector spinae plane; FI: suprainguinal fascia iliaca; RS: rectus sheath; AC: adductor canal; PopSN: popliteal level sciatic nerve.

significant difference in scoring for overall performance highlighting between block regions. However, there was almost universal agreement on the performance of the system for each individual structure (when the assessment was led in a more systematic approach). Further detailed and objective analysis must follow, both in the pre-clinical (e.g. objective assessment of impact on ultrasound image analysis) and clinical environment (e.g. quantitative and qualitative feedback from using it in the peri-operative setting). Determining the risk of the system failing to identify anatomical structures such as an artery or nerve, or mis-identifying a nerve as an artery (or vice versa), is of great clinical significance in UGRA. Failure to identify inadvertent vascular entry with the needle, and consequent intravascular injection of local anesthetic, carries the risk of local anesthetic systemic toxicity (Taylor & Grant, 2019). Similarly, failure to correctly identify nerve tissue may risk nerve trauma by the needle. These factors must be closely scrutinized.

Potential limitations to the system also exist. For example, if the observation that regions containing major vascular landmarks and distinct nerve targets (rather than fascial planes as targets) score more highly is consistent on further assessment, this must be explored. It will be important to determine whether this is due to human input to the system or a performance characteristic of the algorithm. If it represents a deficiency in the algorithm, this must clearly be addressed. Evaluating the performance of anesthesiologists (of varying expertise) in identifying anatomical structures in block regions containing blood vessels, nerves, muscle and bone is similarly important. This may help to determine which regions and structures such assistive technology might provide the most benefit for when performing ultrasound scanning. Validation of this technology will also require study in the pediatric population, in high BMI individuals (e.g. >35 kg/m²), and in the presence of atypical anatomy/pathology distorting the structures highlighted.

Another consideration, when integrating new technology such as this into the applications of clinical anatomy, is the issue of

“trustworthiness”. Clinicians, especially if under-confident in their anatomical knowledge, may over-rely on such assistance. It is therefore important to recognize that all systems have the potential for error and that such technology is not a substitute for robust understanding of the underlying anatomy.

5 | CONCLUSIONS

This paper reports a preliminary evaluation of an assistive AI system which facilitates the recognition of anatomical structures on ultrasound for the purposes of UGRA. It is performed from a clinical viewpoint, with experts in the field rating overall performance of the system, assessing whether highlighting helped identify the relevant anatomical structures and if this would help confirm the correct ultrasound view to a less experienced practitioner. Whilst they must be validated with further study, the results show promise for the accuracy and clinical utility of the system – particularly for nonexperts in UGRA. If “*ultrasound ... has given new life to the appreciation of clinical anatomy*” (Soeding & Eizenberg, 2009), then new technology such as this may enhance the opportunity to energize the field of clinical anatomy and engage clinicians in a discipline for which current evidence indicates that anatomical knowledge is imperfect.

ACKNOWLEDGMENTS

The authors would like to thank Professor Pete Wall for his advice and guidance in undertaking this project.

CONFLICT OF INTEREST

JB & DBSL are Clinical Advisors for Intelligent Ultrasound Limited, receiving honoraria. DBSL is the Lead Clinician on *ScanNav Anatomy Peripheral Nerve Block*. LT is the current Treasurer of Regional Anesthesia UK: views expressed here are personal opinion and do not necessarily reflect the organization LT represents.

AUTHOR CONTRIBUTIONS

James Bowness: manuscript drafting/editing, manuscript submission. Ourania Varsou: data analysis, manuscript drafting/review. Lloyd Turbitt: manuscript drafting/review. David Burkett-St Laurent: study design, manuscript drafting/review.

FINANCIAL DISCLOSURE

This work, undertaken as part of the validation study for medical device regulatory approval, was funded by Intelligent Ultrasound Limited (Cardiff, UK).

ORCID

James Bowness  <https://orcid.org/0000-0002-8665-1984>

REFERENCES

- Alkhatib, M., Hafiane, A., Vieyres, P., & Delbos, A. (2019). Deep visual nerve tracking in ultrasound images. *Computerized Medical Imaging and Graphics*, 76, 101639.
- Bowness, J., El-Boghdadly, K., & Burkett-St Laurent, D. (2020). Artificial intelligence for image interpretation in ultrasound-guided regional Anaesthesia. *Anaesthesia*, 76, 602–607. <https://doi.org/10.1111/anae.15212>
- Bowness, J., Turnbull, K., Taylor, A., Halcrow, J., Chisholm, F., Grant, C., & Varsou, O. (2019a). Identifying the emergence of the superficial peroneal nerve through the deep fascia on ultrasound and by dissection. *Clinical Anatomy*, 32, 390–395.
- Bowness, J., Turnbull, K., Taylor, A., Halcrow, J., Raju, P., Mustafa, A., ... Grant, C. (2019b). Identifying variant anatomy during ultrasound-guided regional anaesthesia: Opportunities for clinical improvement. *British Journal of Anaesthesia*, 122(5), e75–e77.
- Helen, L., O'Donnell, D. B., & Moore, E. (2015). Nerve localisation techniques for peripheral nerve block and possible future directions. *Acta Anaesthesiologica Scandinavica*, 59, 962–974.
- Henderson, M., & Dolan, J. (2016). Challenges, solutions, and advances in ultrasound-guided regional anaesthesia. *BJA Education*, 16(11), 374–380.
- Huang, C., Zhou, Y., Tan, W., Qiu, Z., Zhou, H., Song, Y., ... Gao, S. (2019). Applying deep learning in the recognising the femoral nerve block region on ultrasound images. *Annals of Translational Medicine*, 7(18), 453–459.
- Hutton, M., Brull, R., & Macfarlane, A. J. R. (2018). Regional anaesthesia and outcomes. *BJA Education*, 18(2), 52–56.
- IBM Corp. (2020). *IBM SPSS statistics for windows, version 27.0*. Armonk, NY: IBM Corp.
- Munimara, S., & McLeod, G. (2015). A systematic review and meta-analysis of ultrasound versus electrical stimulation of peripheral nerve location and blockade. *Anaesthesia*, 70, 1084–1091.
- Oh, T. T., Ikhsan, M., Tan, K. K., Rehena, S., Han, N.-L. R., Tiong, A., ... Sng, B. H. (2019). A novel approach to neuraxial anesthesia: Application on an automated spinal landmark identification. *BMC Anesthesiology*, 19, 57–64.
- Ronneberger O., Fischer P., & Brox T. (2015). U-net: Convolutional networks for biomedical image segmentation. arXiv:1505.04597.
- Sites, B. D., Chan, V. W., Neal, J. M., Weller, R., Grau, T., Koscielniak-Nielsen, Z. J., & Ivani, G. (2009). The American Society of Regional Anesthesia and Pain and the European Society of Regional Anaesthesia and Pain Therapy Joint Committee Recommendations for education and training in ultrasound-guided regional Anaesthesia. *Regional Anesthesia and Pain Medicine*, 34, 40–46.
- Smistad, E., Johansen, K. F., Iversen, D. H., & Reinertsen, I. (2018). Highlighting nerves and blood vessels for ultrasound-guided axillary nerve block procedures using neural networks. *Journal of Medical Imaging*, 5(4), 044004.
- Soeding, P., & Eizenberg, N. (2009). Review article: Anatomical considerations for ultrasound-guidance for regional anesthesia of the neck and upper limb. *Canadian Journal of Anesthesia*, 56, 518–533.
- Taylor, A., & Grant, C. (2019). Complications of regional anaesthesia. *Anaesthesia and Intensive Care Medicine*, 20(4), 210–214.
- Tran, D., & Rohling, R. N. (2010). Automatic detection of lumbar anatomy in ultrasound images of human subjects. *IEEE Transactions on Biomedical Engineering*, 57(9), 2248–2256.
- Tremlett M. (2014). Final Fellowship of the Royal College of Anaesthetists (FRCA) Examination Chairman's Report (Academic Year September 2013–July 2014): Review of the RCoA Final Exam 2013–2014.
- Turbitt, L. R., Mariano, E. R., & El-Boghdadly, K. (2020). Future directions in regional anaesthesia: Not just for the cognoscenti. *Anaesthesia*, 75 (3), 293–297.

SUPPORTING INFORMATION

Additional supporting information may be found online in the Supporting Information section at the end of this article.

How to cite this article: Bowness, J., Varsou, O., Turbitt, L., Burkett-St Laurent, D. (2021). Identifying anatomical structures on ultrasound: assistive artificial intelligence in ultrasound-guided regional anaesthesia. *Clinical Anatomy*, 1–8. <https://doi.org/10.1002/ca.23742>